Simulation of Glassy Polymethylene Starting from the Equilibrated Liquid

Richard H. Boyd* and P. V. Krishna Pant

Departments of Materials Science and Engineering and Chemical Engineering, University of Utah, Salt Lake City, Utah 84112

Received November 27, 1990; Revised Manuscript Received February 22, 1991

ABSTRACT: A simulation of glassy polymethylene, as represented by a periodic assembly of 32 chains of 24 methylene units each, was carried out by energy minimization. The starting structures were equilibrium liquid samples taken from a constant-pressure and -temperature Monte Carlo simulation. Volume was allowed to participate in the minimization so that densification and the property changes accompanying it could be studied. The C_{24} methylene system both experimentally and by simulation has a noticeably higher specific volume than long-chain polyethylene, but the fractional degree of densification on quenching to 0 K is in agreement with that for PE. The calculated cohesive energy of both the starting liquid and the glasses were in good agreement with experiment for a C_{24} alkane. The intermolecular radial distribution functions in the glass show much sharper features than those for the liquids and indicate well-developed coordination of neighbors about the methylene units. The distribution of free volume and cavity sizes is discussed. The mechanical elastic properties of the glasses were also derived from the calculated compliance constant matrix. The derived shear modulus for the C_{24} glass, at the density from simulation, is somewhat lower than that found experimentally from extrapolations for semicrystalline PE. However, when calculated at the density of high molecular weight PE, the agreement is much better.

Introduction

The process of vitrification and the structure and properties of polymeric glasses are subjects of long-standing interest in polymer science. Recent progress in the ability to simulate polymeric liquid structures makes it possible to undertake the study of glass formation and glass structure. Molecular dynamics (MD) has been used in this context.[1-3] In spite of the inherently short time trajectories (up to ~1 ns), presently practical computationally in MD, the strong temperature dependence of segmental motion makes it possible to generate liquid structures at temperatures not greatly higher than the glass temperature. Monte Carlo (MC) simulation is also a viable method for liquid structure generation.[4,5] In our own work we have carried out a MC simulation of polymethylene under the conditions of constant pressure.[5] The model is sufficiently realistic that the P–V–T results, i.e., the specific volume as a function of temperature and pressure, could be compared favorably with experiment.

The formation of a glass in simulations can be approached several ways. In MD the temperature is simply lowered to where the segmental motion (bond rotations) is frozen out in runs of the same time scale as those that produced a liquid structure at higher temperature.[1-3] Another approach is to use energy minimization to generate the glass. Without advocating one method over the other, it is useful to make some comparisons. Both methods have a great deal in common. Energy minimization finds a structure that is locally minimum and makes no attempt to find the global one (the crystalline state where regular chemical structure allows). The short time scales of MD effectively result in the same thing, although the effect of temperature on the structure about the local minimum is included. If energy minimization is thought of as a gradient, steepest descent method with small steps, then it corresponds to MD carried out near 0 K (zero kinetic energy and vanished acceleration term). Both methods capture what is commonly presumed to be the essence of glass formation. That is, they find a local structure, quiescent in major segmental rearrangements, that is lower in energy and reachable from the liquid by relatively minor structural adjustments. Due to the relatively short MD time trajectories, neither method addresses effectively a subject of major interest, the time dependence of the structural adjustments, especially when the latter are long term, of the order of hours and longer. Physically, the processes simulated can be thought of in energy minimization as a fast quench to 0 K from the liquid and in MD as a fast quench to a finite temperature from the liquid. In the present work, we study glasses of polymethylene prepared by energy minimization from equilibrated liquids, the latter having been generated by MC simulation. It differs from previous energy minimization preparations of glasses[6-8] in that the changes in structure on glass formation from the liquid are addressed rather than generating the packing entirely by this method.

Densification is one of the central features of vitrification. Thus in the study of glasses via simulation it is very important that the effect of volume change be considered. In the present work we use a formulation of energy minimization that explicitly includes the system volume.[9] This is accomplished by including the periodic box dimensions as variables in the energy function. They are optimized simultaneously with the atom positions in minimization. Since the energy minimization corresponds to a quench to 0 K process, we will consider the volumes calculated to be 0 K volumes for the glass.

Calculations

The structural model for the polymer chain is similar to that used previously.[5] In order to use a respectably large system of chains and chain atoms, the hydrogens on the methylene unit are contracted into "united atom" methylene beads. The Lennard-Jones potential for CH_2...CH_2 nonbonded interactions previously used was invoked as well as the torsional potential. In addition, as it was felt that the internal valence coordinate changes on densification should be of interest, functions for bond length and valence angle distortions[10] were included as well. All of the potential function parameters are summarized in Table I. The systems were comprised of 32 chains of 24 methylene units each or 768 total methylene units. The starting structures were generated by MC simulation as previously described.[5,11] Energy minimization was carried

0024-9297/91/2224-4078$02.50/0

Table I
Potential Functions[a]

function	constants
harmonic bond stretch = $(1/2)k_R(R - R_0)^2$	$k_R = 2650$, $R_0 = 1.54$
harmonic bond bending = $(1/2)k_\theta(\theta - \theta_0)^2$	$k_\theta = 482$, $\theta_0 = 111.6°$
torsional potential = $(1/2)V_1(1 + \cos\phi) + (1/2)V_3(1 + \cos 3\phi)$	$V_1 = 3.35$, $V_3 = 13.4$
nonbonded potential, Lennard-Jones 6-12	$\epsilon = 0.495$, $R_{min} = 4.335$, $\sigma = 3.862$

[a] Energies are in kilojoules per mole, distances in angstroms, and angles in radians (shown above in degrees).

out via the Newton-Raphson method, with the volume optimized simultaneously with atom coordinates, as described in the preceding paper.[9] In computing intermolecular nonbonded energies, summations were carried out to 9 Å. In addition, a truncation correction was carried out as previously described.[5] These contributions are listed separately in our results. Its inclusion greatly enhances the accuracy of comparisons with experimental energy related quantities.

Five snapshots from MC runs at each of three temperatures, 300, 350, and 400 K, were energy minimized. The compliance matrices for periodic box a-c degrees of freedom were also calculated for each minimized snapshot. In order to study the effects of vibrational degrees of freedom separately from changes in packing on densification, the MC snapshots at 300 K were energy-minimized constrained at the original liquid volume of each in addition to carrying out the minimization with box dimensions and thus volume participation.

Results

Several issues are of interest. One is the degree of densification achieved and whether or not it depends on the starting state either through the particular snapshot minimized or more importantly through the temperature of the initial system. The same applies to the enthalpy change and how the latter is distributed over the molecular degrees of freedom. The structural or packing changes, including measures of free volume are of interest as well. Finally the mechanical properties as derived from the compliance constants are pertinent. Where possible, we attempt to compare the simulation results with experiment.

Specific Volume. The volumes of the starting MC systems and their derivative volume optimized energy-minimized, 0 K, states are listed in Table II. The relation of the liquid volumes and the 0 K glasses to the temperature scale is better visualized as in Figure 1. The liquid volumes have already been shown to agree well with experiment (~2%) for the C_{24} hydrocarbon, tetracosane, for which the simulation is appropriate. Polyethylene (PE) is noticeably more dense, ~5%, than hydrocarbon chains of this length. An estimate of the volume of glassy PE at 0 K can be made, but the results need to be corrected for the finite chain length effect of the simulation. We do this by comparing V_T/V_0, the ratio of the volumes at liquid temperature T, to the 0 K volume for PE and the simulation. The effect of finite chain length should be much greater on the absolute volumes than on the volume changes with temperature. The experimental values for V_T/V_0 were derived as follows. Stehling and Mandelkern[12] have measured thermal expansions of PE's of varying crystallinity down to -195 °C. By extrapolating their results vs crystallinity, we find for amorphous PE that $V(-120\ °C) = V(25\ °C)/1.108$ and that $V(-195\ °C) = V(-120\ °C)/1.028$. From linear extrapolation through -120 and -195 °C, we estimate $V(-273\ °C) = V(-195\ °C)/1.02$. Choosing $V(25\ °C) = 1.18\ cm^3/g$[13] leads to $V(-120\ °C) = 1.065\ cm^3/g$, $V(-195\ °C) = 1.035\ cm^3/g$, and $V(-273\ °C) = 1.015\ cm^3/g$. It is difficult to judge the accuracy of these results; they are intended to be expressed to ~1/2%, 0 or 5 in the last place. The overall uncertainty could be greater. The ratios V_T/V_0 thus found for PE are shown in Figure 2 along with the average values from the simulations. It may be seen that the simulation does a creditable job of representing the densification accompanying glass formation.

Enthalpy. A summary of the distribution of energy over the various degrees of freedom for the energy-minimized systems is given in Table III.

We address the degree to which the cohesive energy calculated agrees with experiment. This can be done for both the liquid and for the 0 K glass. The experimental heat of vaporization of the C_{24} alkane, tetracosane, can be derived from tabulated heats of vaporization of lower liquid alkanes. From data in Stull et al.[14] we find that the equation

$$\Delta H_{vap}(exp) = 2.090 + 4.928n \quad (1)$$

fits the heats of vaporization as a function of the carbon number, n, very well. Thus for $n = 24$ $\Delta H_{vap}/CH_2 = 5.01$ kJ/mol. In the simulation, the heat of vaporization consists of the change in nonbonded and torsional energy on vaporization and in principle the change in vibrational energy associated with the bond stretching and bending degrees of freedom as well. These were not included in the liquid simulation (although they were for the glass). Since the simulation is a classical one, the energies would not be appropriate since these degrees of freedom have not become classical yet. However, it should be a very good approximation to regard the internal vibrational energy as the same in both the liquid and the vapor. The torsional energy can be thought of as made up of two terms. One is the vibrational energy above the local trans and gauche minima, and the other is the contribution due to the population of the gauche states, which have their minima above the trans. Under the approximation of the vibrational energies being the same, this leaves the energy difference between the liquid and vapor as the change in nonbonded energy plus that due to any change in the relative population of the gauche and trans states on vaporization. It is expected that the gauche/trans population should be the same under both conditions. This was confirmed by comparing the simulation values for the gauche/trans ratio in the liquid with a rotational isomeric state calculation of the population. The latter should be appropriate for the isolated molecule condition in the vapor. Thus the simulation value for the heat of vaporization should be just the negative of the intermolecular nonbonded energy ($+RT$). The liquid simulations[5] at 300 K gave an average value for the intermolecular energy of -4.9 kJ/mol or $\Delta H_{vap}/CH_2(calc) = 5.0$ kJ/mol. This is in, no doubt in some degree fortuitous, exact agreement with the experimental value (Table IV).

The cohesive energy of the 0 K glass was defined here as the energy change on vaporizing the glass to a state V', where the conformation states of the chains are the same as those in the glass. A thermodynamic cycle relating this state change to experimentally accessible quantities is shown in Figure 3. From simulation there is found to be very little change on quenching in the conformational states with respect to classification as trans versus gauche.

Table II
Specific Volumes of Initial and Minimized Systems

	specific vol, cm³/g		box size			V_T/V_0	
T(initial), K	initial	0 K	a, Å	b, Å	c, Å	calc	exptl[a]
300	1.216	1.068	27.09	26.68	26.59		
	1.212	1.069	27.26	26.86	26.59		
	1.209	1.068	26.53	26.82	27.01		
	1.245	1.063	26.43	26.04	27.82		
	1.228	1.075	26.61	26.11	27.83		
average	1.222 ± 0.013	1.069 ± 0.004	26.78	26.50	27.17	1.14	1.17
350	1.273	1.063	26.59	27.39	26.29		
	1.270	1.070	26.87	26.89	26.66		
	1.240	1.078	26.54	27.13	26.96		
	1.257	1.066	25.63	27.36	27.37		
	1.245	1.075	26.75	27.54	26.26		
average	1.257 ● 0.013	1.070 ± 0.005	26.48	27.26	26.71	1.17	1.20
400	1.329	1.071	26.27	27.72	26.48		
	1.338	1.076	25.84	27.70	27.06		
	1.314	1.083	26.07	27.96	26.75		
	1.297	1.066	25.59	28.98	25.89		
	1.319	1.069	27.38	25.27	27.88		
average	1.319 ± 0.014	1.073 ● 0.006	26.23	27.52	26.81	1.23	1.24

[a] For PE, see text.

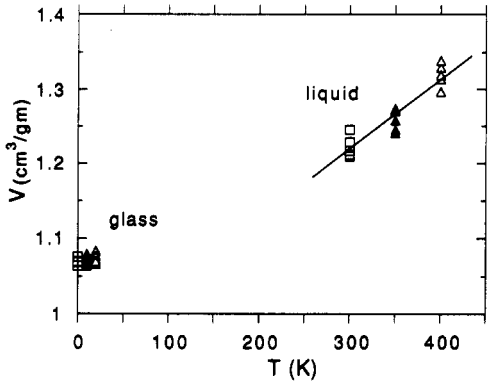

Figure 1. Specific volume from simulation. Five samples at each of three starting temperatures, 300 K (open squares), 350 K (filled triangles), and 400 K (open triangles), for the liquids were used. The same symbols are used for the 0 K energy-minimized glasses derived from the liquids. The latter are offset in the plot from 0 K for clarity.

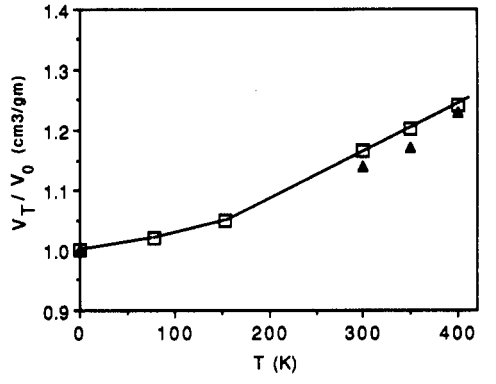

Figure 2. Fractional increase in specific volume at T (K) relative to 0 K from simulation (average values; filled triangles) compared to experiment for polyethylene (open squares).

Table V summarizes the effect of quenching on torsional angle classification. Thus, the hypothetical 0 K vapor, V', can be taken to have the same gauche/trans composition as the 298 K vapor, V. The experimental enthalpy change for step 1, the change in the 0 K glass in going to the liquid at 298 K, was taken to be the same as that for long-chain polyethylene. Chang[15] has extrapolated the thermodynamic functions of semicrystalline PE to the amorphous condition and gives the value $H_{298} - H_0 = 4.5$ (kJ/mol)/CH_2. It is not known how much difference there would be between the long-chain value and that for our C_{24} simulation although the chain-length effect is presumably small. The enthalpy change for step 2 is the experimental heat of vaporization and is 5.0 kJ/mol. The enthalpy change for step 3 in Figure 3 is the vibrational (+ rotation + translation for whole molecules) enthalpy change in going from V to V'. This change was calculated as described before[5] by selecting several chains from the simulated liquid and placing explicit hydrogens on them. Then these chains were subjected to vibrational analysis and the thermodynamic functions derived. This leads to −3.7 (kJ/mol)/CH_2 for this step. Although this is not strictly an experimental value, the only significant error involved is that from anharmonic effects on the vibrations. These should be negligible at the accuracy required here. Summing steps 1–3, the experimental cohesive energy is found to be 5.8 (kJ/mol)/CH_2 (Table IV). The simulation value for the cohesive energy is the intermolecular nonbonded energy at 0 K. The latter is, from Table III, equal to 6.0 (kJ/mol)/CH_2. Thus there is also very good agreement between the experimental and calculated cohesive energies for the glass (Table IV).

There are two major effects on quenching (energy minimization). One is the removal of most of the energy associated with the vibrational degrees of freedom. The other is the optimization of the packing that accompanies the densification. To some degree, these effects can be studied separately by the device of energy minimizing at the fixed volume of the liquid and comparing the results with the volume-optimized energy minimization. The fixed-volume quench removes vibrational energy but does not effect the packing and structural changes that accompany densification. Table VI shows the energy changes for the various degrees of freedom in going from minimized systems at the liquid volume at 300 K to those at optimized volume. Thus these are the changes associated with densification and packing optimization. The *positive* changes in the stretching, bending, torsional, and intramolecular energies to be seen are those that result in order to *lower* the intermolecular nonbonded energies and thus arrive at an overall energy minimum. It may be seen that the average total energy change on densification of −335 (kJ/mol)/system is made up of a decrease of −492 (kJ/mol)/system in the intermolecular packing energy and an increase of 157 (kJ/mol)/system in the intramolecular degrees of freedom. Thus the change in total energy due

Table III
Energy Distribution in 0 K Glasses[a]

	intramolecular degrees of freedom					intermolecular degrees of freedom			
	stretch	bend	torsion	nonbond	subtotal	nonbond	trunc[b]	subtotal	total
T(initial) = 300 K	7.5	63.2	760.4	-508.9	322.1	-4090.3	-580.2	-4670.4	-4348.3
	7.6	65.3	860.4	-491.2	442.2	-4079.6	-579.3	-4658.9	-4216.7
	6.9	71.6	861.8	-511.4	428.9	-4070.0	-580.1	-4650.8	-4221.1
	6.7	57.3	921.0	-484.3	500.6	-4104.8	-582.2	-4686.9	-4186.4
	6.6	73.3	911.9	-491.9	499.9	-4061.3	-576.4	-4637.7	-4137.8
average	7.0	66.1	863.1	-497.5	438.7	-4081.2	-579.6	-4661.0	-4222.1
T(initial) = 350 K	7.3	63.7	978.2	-514.3	534.8	-4049.4	-582.0	-4631.5	-4096.7
	7.2	59.6	987.4	-542.0	512.3	-4000.4	-578.5	-4578.9	-4066.6
	7.2	58.4	1010.5	-523.9	552.2	-4003.0	-574.1	-4577.1	-4024.9
	6.5	65.0	954.8	-509.9	516.6	-4047.1	-580.7	-4627.8	-4111.3
	7.2	55.5	977.0	-504.5	535.2	-4034.7	-576.0	-4610.7	-4075.6
average	7.1	60.4	981.6	-518.9	530.2	-4026.9	-578.3	-4605.2	-4075.0
T(initial) = 400 K	6.6	67.2	1145.0	-564.3	654.5	-3937.3	-578.0	-4515.4	-3860.8
	6.8	63.9	1101.8	-511.1	661.4	-4012.9	-575.4	-4588.4	-3926.9
	6.9	54.1	1066.5	-531.9	595.7	-3930.5	-571.8	-4502.2	-3906.5
	6.4	72.0	1122.1	-544.3	656.2	-4021.0	-580.9	-4610.9	-3945.6
	6.9	72.5	1053.6	-529.2	603.8	-3995.3	-577.9	-4573.2	-3969.4
average	6.7	65.9	1097.8	-536.1	634.3	-3979.4	-576.8	-4556.2	-3921.9

[a] Energies are in kilojoules per mole per periodic box; there are 24 × 32 = 768 methylene units per box. [b] Truncation correction to intermolecular nonbonded energy.

Table IV
Comparison of Calculated and Experimental Enthalpies[a]

	heat of vaporization		cohesive energy	
	simulation	exptl	simulation	exptl
liquid, 298 K	5.0	5.01		
0 K glass			6.0	5.8

[a] Units are in kilojoules per mole per CH_2. Both simulated and experimental values are for C_{24} alkane; see text.

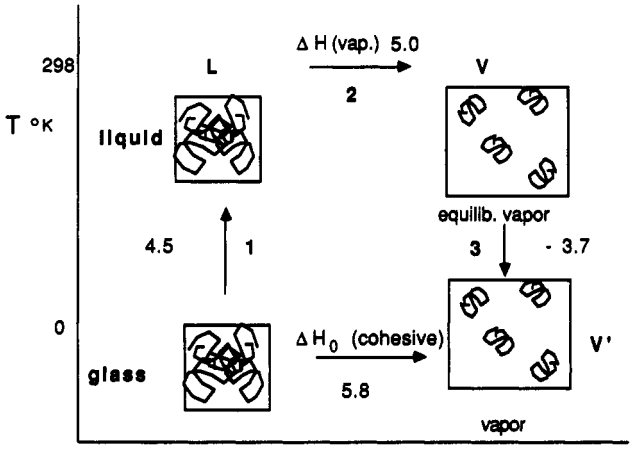

Figure 3. Thermodynamic cycle for determination of the experimental cohesive energy of polyethylene glass. Values for the steps are in kilojoules per mole per CH_2.

Table V
Torsional Angle Distribution in Glass vs Liquid

T(initial), K	liquid			glass			torsional[a] transitions, %
	T %	G %	G′ %	T %	G %	G′ %	
300	68	16	16	68	17	15	6.6
350	65	17	18	65	18	17	8.9
400	63	18	19	62	19	19	8.8

[a] Percentage of bonds that changed classification among trans (120° < T < 240°), gauche (0° < G < 120°), and gauche′ (240° < G′ < 0°) during minimization.

to packing optimization on densification is ~0.5 (kJ/mol)/CH_2. This is on the order of 10% of the cohesive energy of the glass [6 (kJ/mol)/CH_2].

It was seen that there is no significant effect of the starting volume on the volume achieved on quenching (Table II). In Table III it is apparent that there is an effect on the torsional energy of the starting temperature that carries over into the total energy. This is an expression of the fact that the quench traps the chains in the conformations of the liquid and very few bond conformational changes that can be classified as gauche to trans or vice versa take place. Thus, after the removal of the vibrational torsional energy there still remains the contribution of the gauche state minima relative to the trans. The higher energy for the glass quenched from higher temperature reflects the higher gauche populations in the starting liquid.

Structure. A commonly used probe of the structural features of glasses and liquids is the radial distribution function. In our case we are mainly interested in the features associated with intermolecular packing. Thus, it is appropriate to accumulate separately during sampling an intermolecular radial distribution function. The function is expressed as number density, (number of methylene centers)/Å^3, and was accumulated by counting the number of centers, not in the same molecule, in a spherical shell of thickness ΔR = 0.1 Å at a distance R from the selected central unit, dividing by $4\pi R^2\Delta R$, and averaging the result over all methylene units as the central unit. Thus the function times ΔV (in Å^3) for a volume element at distance R (in Å) gives the number of centers not in the same molecule in ΔV. Figure 4 shows comparisons of the intermolecular radial distribution function of the liquid with that for the 0 K glass derived from it, for a snapshot for each of the three starting temperatures. For the liquids it may be seen that the main features are the onset of neighbors at about 3.3 Å and a broad maximum at about 5.2 Å. The latter feature represents a first neighbor interchain distance. There is evidence of a shoulder at about 4.0 Å. In the glasses, not surprisingly, the features are much sharper. The onset of neighbor contacts is very abrupt at 3.6 Å and a distinct maximum, rather than a weak shoulder, now occurs at 4.0 Å. The repulsive diameter of the methylene spheres as measured by the Lennard-Jones "σ" parameter, from Table I, is 3.86 Å. Thus, it is apparent that close contact of the CH_2 beads is a prominent feature of the packing in the glass. Integration of the radial distribution function from 3.6 Å up to the maximum at 4.0 Å gives an occupancy of 2.4 methylene units. Assuming contacts of this type to be symmetrical about the maximum, this indicates a coordination number of 4.8

Table VI
Energy Changes from 300 K Minimized Systems to 0 K Minimized[a]

	intramolecular degrees of freedom					intermolecular degrees of freedom			
	stretch	bend	torsion	nonbond	subtotal	nonbond	trunc[b]	subtotal	total
	5.6	33.7	104.4	-9.3	134.4	-459.0	-71.2	-530.2	-395.9
	5.9	35.9	166.3	11.7	219.8	-421.6	-68.5	-490.1	-270.4
	5.2	40.8	163.8	-12.7	197.2	-416.2	-68.0	-485.0	-287.8
	3.8	25.9	121.8	0.2	151.7	-393.7	-84.8	-478.6	-326.8
	4.4	34.7	46.9	-0.1	85.8	-406.5	-72.2	-478.7	-392.9
average	4.9	34.2	120.6	-0.2	157.7	-419.4	-73.0	-492.5	-334.7

[a] Energies are in kilojoules per mole per periodic box; there are 24 × 32 = 768 methylene units per box. [b] Truncation correction to intermolecular nonbonded energy.

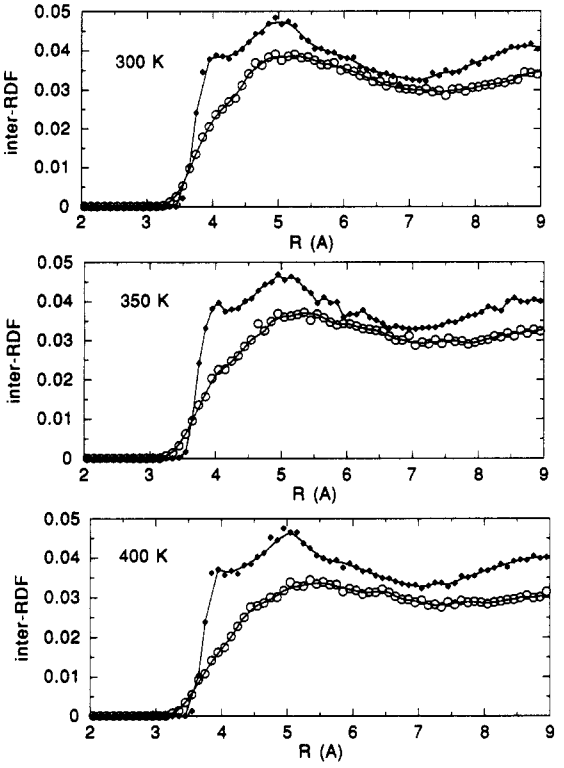

Figure 4. Intermolecular radial distribution functions, expressed as number density (particles/Å^3), from simulation compared for liquids at the temperature indicated (open circles) and the 0 K glasses (filled diamonds) derived from them.

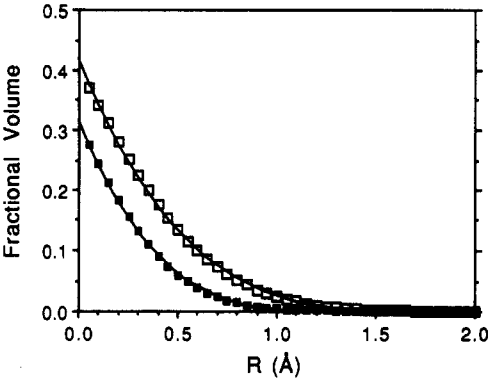

Figure 5. Fraction of the system volume available to a probe sphere as a function of the radius of the sphere for a 300 K liquid (open squares) compared to the corresponding glass (filled squares).

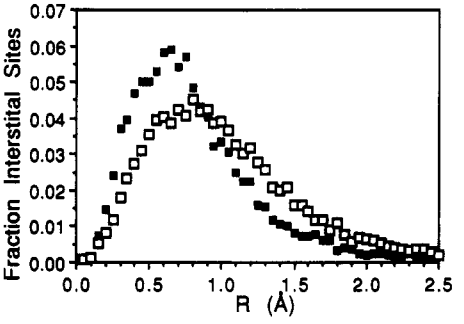

Figure 6. Distribution of cavity sizes, as measured by inscribing an interstitial probe sphere, versus sphere radius for a 300 K liquid (open squares) compared to the corresponding glass (filled squares).

for the methylene unit intermolecular contacts in the glass.

A concept that has been widely invoked in the study of glasses is that of free volume. The amount of free volume obviously depends on the definition of the occupied volume. We take the latter here as being defined by the "σ" repulsive diameter of the methylene spheres. The unoccupied volume is then easily sampled by placing points at random and checking them for being outside of occupied spheres. The fraction of points placed that are in free space is the fractional free volume. The distance to the nearest occupied sphere represents the radius of the largest probe sphere that will fit at the selected point in open space. Since all smaller probe spheres will also fit at the point, the integral of the distribution of largest probe sphere distances represents the fraction of free volume available to spheres of varying radius. Figure 5 shows this distribution for both the 300 K liquid and the 0 K glass prepared from it. Its features are very similar for both cases, there obviously being greater fractional free volume in the liquid. This distribution tells relatively little about the actual sizes of holes or cavities in the structure. The largest probe sphere that can be inscribed in an open space (and is not restricted to being about a previously selected fixed point) touches four occupied methylene spheres and thus is a tetrahedrally coordinated interstice. We have described the determination of an approximate distribution function for the sizes of tetrahedrally coordinated interstices.[11] Figure 6 compares the distributions for hole sizes determined this way for the 300 K liquid and its 0 K glass. The distribution is more sharply peaked and has a somewhat smaller peak value radius in the glass. Figure 7 compares the cavity size distributions among glasses prepared from the three initial temperatures. There appears to be no discernible effect of the starting temperature on the distribution.

Mechanical Properties. The compliance matrices for tensile variations of the box dimensions a–c calculated for the glasses are displayed in Table VII. Engineering moduli were calculated from the compliance matrices using the following relations. The tensile modulus, E, is reported as the average of S_{aa}^{-1}, S_{bb}^{-1}, and S_{cc}^{-1}. The Poisson's ratio uses the average of S_{aa}, S_{bb}, and S_{cc} for S_{aa} and the average of S_{ab}, S_{ac}, and S_{bc} for S_{ab} in $\nu = -S_{ab}/S_{aa}$. The shear modulus, G, is given in terms of the isotropic tensile modulus and Poisson's ratio by $G = (1/2)E/(1 + \nu)$. The isothermal compressibility is given by $\beta = \sum_{ij} S_{ij}$ and the

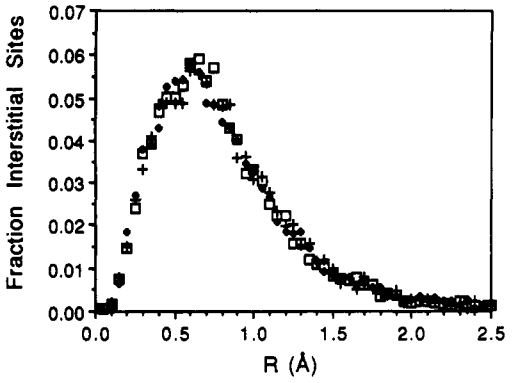

Figure 7. Distribution of cavity sizes, as measured by inscribing an interstitial probe sphere, versus sphere radius compared for glasses prepared from the initial temperatures of 300 K (open squares), 350 K (filled diamonds), and 400 K (crosses).

Table VII
Calculated Compliance Matrices, S_{IJ}, of 0 K Glasses[a]

T(initial), K	I	$J = 1$	$J = 2$	$J = 3$
300	1	0.531 ± 0.102	−0.207 ± 0.051	−0.225 ± 0.039
	2	−0.207 ± 0.051	0.480 ± 0.085	−0.188 ± 0.078
	3	−0.225 ± 0.039	−0.188 ± 0.078	0.470 ± 0.081
350	1	0.556 ± 0.075	−0.221 ± 0.037	−0.222 ± 0.038
	2	−0.221 ± 0.037	0.431 ± 0.048	−0.155 ± 0.032
	3	−0.222 ± 0.038	−0.155 ± 0.032	0.446 ± 0.073
400	1	0.690 ± 0.342	−0.237 ± 0.214	−0.374 ± 0.381
	2	−0.237 ± 0.214	0.679 ± 0.320	−0.349 ± 0.072
	3	−0.374 ± 0.381	−0.349 ± 0.072	0.790 ± 0.354

[a] Units are GPa^{-1}. 1, 2, and 3 refer to the a–c directions of the periodic box. Plus/minus refers to standard deviation for the five snapshots minimized for each initial temperature.

Table VIII
Average Mechanical Properties of 0 K Glasses

T(initial), K	tensile modulus, GPa	Poisson's ratio	isothermal compressibility, GPa^{-1}	bulk modulus, GPa	shear modulus, GPa
300	2.02	0.42	0.24	4.1	0.71
350	2.09	0.42	0.24	4.2	0.74
400	1.39	0.44	0.24	4.1	0.48
at 0 K PE volume[a]	4.07	0.40	0.15	6.7	1.46

[a] Calculated at the experimental specific volume of high molecular weight amorphous PE, =1.01 cm^3/g, rather than at the specific volume of C_{24} alkane determined from simulation.

bulk modulus by $B = \beta^{-1}$. These quantities are given in Table VIII.

Comparison with experiment is possible, in principle, by extrapolation of low-temperature mechanical data for semicrystalline PE versus crystallinity. Probably the best data are measurements of the shear modulus over a wide crystallinity range by Illers.[16] Extrapolation to zero crystallinity gives a shear modulus at 90 K, below the γ relaxation, of ~2 GPa. This is considerably higher than the calculated values of ~0.7 GPa. A possible source of discrepancy is the finite chain effect. In the enthalpy comparisons above where good agreement was obtained, finite chain alkane experimental data could be largely used. But this is not possible in the present case, and, as discussed above, both the experimental and calculated specific volumes are higher for the C_{24} chains than for long-chain PE. The calculated glass volumes are ~6% higher for the C_{24} chains than for PE. To explore this effect further, additional minimizations were carried out with the volume fixed at the experimental value for PE, 1.01 cm^3/g. Compliance matrices calculated from these systems lead to the results in the last row in Table VIII. It is seen that the results are in fact quite sensitive to the specific volume. The shear modulus is now ~1.5 GPa and in much better agreement with experiment.

Acknowledgment. We are indebted to the Polymers Program, Division of Materials Research of the National Science Foundation, for financial support and to the Utah Supercomputing Institute where the computations were carried out.

References and Notes

(1) Rigby, D.; Roe, R. J. *J. Chem. Phys.* **1987**, *87*, 7285.
(2) Rigby, D.; Roe, R. J. *J. Chem. Phys.* **1988**, *89*, 5280.
(3) Rigby, D.; Roe, R. J. *Macromolecules* **1989**, *22*, 2259.
(4) Vacatello, M.; Avitabile, G.; Corradini, P.; Tuzi, A. J. *J. Chem. Phys.* **1980**, *73*, 548.
(5) Boyd, R. H. *Macromolecules* **1989**, *22*, 2477.
(6) Theodorou, D. N.; Suter, U. W. *Macromolecules* **1985**, *18*, 1467.
(7) Theodorou, D. N.; Suter, U. W. *Macromolecules* **1986**, *19*, 139.
(8) Theodorou, D. N.; Suter, U. W. *Macromolecules* **1986**, *19*, 379.
(9) Boyd, R. H.; Pant, P. V. K. *Macromolecules*, preceding paper in this issue.
(10) Boyd, R. H.; Brietling, S. M. *Macromolecules* **1974**, *7*, 855. The C–C–C bend constant used there was lowered to 0.8 mdyn/Å here, a more realistic value.
(11) Boyd, R. H.; Pant, P. V. K. In *Computer Simulation of Polymers*; Roe, R. J., Ed.; Prentice-Hall: Englewood Cliffs, NJ, 1991.
(12) Stehling, F.; Mandelkern, L. *Macromolecules* **1970**, *3*, 242.
(13) Maloney, D. P.; Prausnitz, J. M. *J. Appl. Polym. Sci.* **1974**, *18*, 2703. Calculated from eq 1 of this paper.
(14) Stull, D. R.; Westrum, E. F., Jr.; Sinke, G. C. *The Chemical Thermodynamics of Organic Compounds*; Wiley: New York, 1969.
(15) Chang, S. S. *J. Res. Natl. Bur. Stand., Sect. A* **1974**, *78A*, 387.
(16) Illers, K. H. *Kolloid Z. Z. Polym.* **1973**, *251*, 394.